

Comprehensive studies of patinas on Renaissance bronze statuettes with laboratory, synchrotron and neutron-aided techniques

JAAP J. BOON*

JAAP Enterprise for Art Scientific Studies
Amsterdam, The Netherlands
molartadvice@jaap-enterprise.com

ROBERT VAN LANGH

Rijksmuseum
Amsterdam, The Netherlands
R.van.Langh@rijksmuseum.nl

*Author for correspondence

KEYWORDS: Renaissance bronzes, patina, imaging microanalysis, x-ray tomography, botryoidal nodules, EDX mapping

ABSTRACT

The spatial distribution of constituents in the patina of Renaissance hollow bronze statuettes adds a new dimension to bulk microanalytical data. Studies of the chemical stratigraphy of patina on bronze statuettes reveal interesting composites consisting of primary layers reflecting dezincification, secondary layers with botryoidal copper sulphate structures and applied organic layers with a chaotic internal structure. To characterize the patina structure fully, various macro and microanalytical 2 and 3-D imaging approaches are combined. Intact patinas have intricate secondary layers developed from mineralising copper metal soaps that suggest a period of slow development. Further organic-rich layers seal and preserve these layers in protected areas of the statuettes, for example in the hair. The absence of these secondary layers changes not only the quality of the patina but may also be an indication of questionable authenticity and/or invasive repairs.

INTRODUCTION

A large body of knowledge is available on the corrosion chemistry of outdoor bronzes and bronze archaeological artefacts (Scott 2002). Much less is known about the construction and chemical composition of indoor Renaissance hollow bronze statuettes. These bronzes are historically important and economically highly valued works of art. Their attribution is predominantly done on the basis of stylistic features (Pope-Hennessy 1965). Patinas on these bronzes are highly appreciated and a key factor in appearance, but little is known about their chemical composition or how they are formed. This paper presents a brief account of a comprehensive approach to the analysis of the chemical stratigraphy of patinas with the goal to learn more about original material composition, the interaction between applied materials and the metal, and the combined effects of ageing and conservation.

The art of manufacturing hollow bronze statuettes using the lost wax technique has continued from the Renaissance until today; thus, it is difficult to determine exactly in which century a bronze has been made. Recent studies using neutron imaging elucidate their manufacturing process (Van Langh et al. 2009, Van Langh 2012). Neutron diffraction imaging gives information about their metallurgy. An underutilised source of information is the external patina, a skin of multilayered material that results from preparation of the metal surface after casting. An application of organic and presumably inorganic materials, the interaction of applied materials with the metal, the interaction with the environment (i.e. moisture, carbon dioxide, sulphur dioxide and other gases), the effects of ageing (which allows slow chemical processes to stabilize the multilayer system), wear and tear, and, finally, various conservation methods all contribute to the patinas' stratigraphy and may be a useful way to determine the possible age of a statuette. Such knowledge can become a powerful tool in the authentication process of Renaissance bronze statuettes, since their patinas have rarely been removed. Earlier studies (Pitthardt et al. 2011) on patinas of indoor Renaissance bronzes give information on the overall composition, but not on the stratigraphy of the patina layer that is investigated here.

EXPERIMENTAL APPROACH

The authors' approach has been to examine and image the surface layers using digital microscopy with a Hirox 3-D digital microscope for the

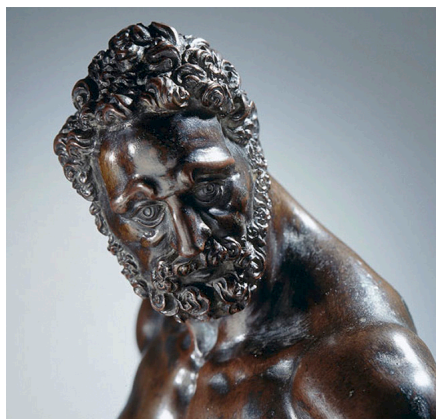


Figure 1

The face and shoulders of *Hercules Pomarius* (BK-1954-43). Microsamples for patina research were removed from the hair

external survey of the surface of the bronzes. The surface layers and loss of layers in some places were visualized and linked where possible to the microstratigraphy. Several statuettes from the 17th and 19th centuries in the collection of the Rijksmuseum were studied. This paper reports on the patinas from two bronzes, *Striding Warrior* (BK-1959-3) and *Hercules Pomarius* (BK-1954-43; c. 1568), both attributed to Willem van Tetrode (1525–80). In both cases, microsamples were taken for chemical stratigraphic analysis from the hair, which is the most likely place for the original patina to remain preserved (Figure 1).

Direct temperature-resolved mass spectrometry (DTMS) was used to determine the organic constituents of the patinas. Small crumbs of the patina intended for cross-section analysis were first studied with scanning electron microscopy (SEM) equipped with energy-dispersive x-ray spectroscopy (EDX), then embedded in Technovit LC2000 and polished using a MOPAS hand-polishing device¹ on micromesh cloths (progressively 1800, 3200, 4000, 6000 and 8000 mesh). Fourier transform infrared microscopic imaging (micro-FTIR) applied in this stage gave information on the distribution of the organic phases and inorganic materials in the layer structure. Cross-section surfaces were covered by cold sputtering with 1.5 nm gold before imaging with an FEI XL-30 FSEM equipped with a nitrogen-cooled EDAX energy-dispersive spectrometer for EDX analysis. Further details on the mineral composition of a patina from the *Hercules Pomarius* were obtained by micro-XRF and micro-XRD imaging on the SLS synchrotron² micro-XAS beamline of a thin section, allowing elemental XRF mapping in combination with micro-x-ray diffraction. The TOMCAT beamline at SLS was used to obtain 3-D x-ray tomographic data on the distribution of the patina on the metal bearer from a hair sample of the *Striding Warrior*.

PATINA ON HERCULES POMARIUS

Microanalytical data

DTMS at low electron voltage is a microanalytical technique in which the homogenized sample is resistively heated in the source of a mass spectrometer. Compounds appear in different temperature windows and their mass spectral features can be correlated with their molecular composition (Boon 1992). A sample from the hair of *Hercules* was found to contain beeswax and carnauba wax, fatty acids like metal soaps with a chain length of 14, 16 and 18 carbons, azelaic acid, molecular fragments of cross-linked oil and synthetic resin (m/z 192, 202). At a higher temperature, the emission of CO_2 , SO_2 and S_2 pointed to decarboxylation of fatty substances, carbonates, sulphates and sulphides. Elemental copper, zinc and a small amount of lead (drier?) were also observed.

FTIR performed on the cross section resulted in an overall FTIR spectrum and individual compound feature maps shown later. Fatty components like waxes and fatty acyl moieties showed CH vibrational features at 2924 and 2854 cm^{-1} . Stretch vibrations from carboxylates linked to Zn and Cu appeared in the 1520–1616 cm^{-1} absorption window. A strong signal in the 1086–1218 cm^{-1} region pointed to sulphates. The FTIR absorption

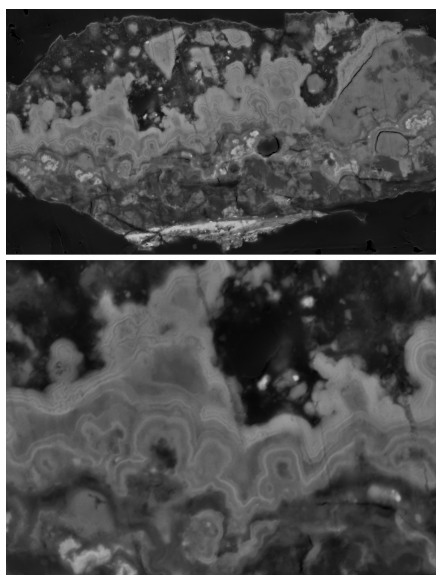


Figure 3

Electron back-scattered (SEM-BSE) images of a polished cross section and detail (lower image) from the hair of *Hercules Pomarius*. Three zones are discerned: a primary less-structured zone on the bronze, a secondary banded crystalline zone and a chaotic third zone rich in waxes and debris

for carbonate at 1405 cm^{-1} was very low, pointing to a virtual absence of carbonates. Imaging maps of these FTIR features in reflection mode were extracted and compared to the SEM image of the cross section.

Scanning electron microscopy of sample particles mounted directly on a stub with carbon sticky tape showed a great variety of surface features and elemental compositions. Often, open broken areas of the patina allowed a first view into the buildup of the patina. EDX probing of these layers gave indications of the organic or inorganic nature of the layers. Organic crystals of paraffin or wax are not uncommon and form complicated crystalline nets over the patina surface (Figure 2A). Some samples showed evidence of filaments of bacteria or fungi where the patina and metal come into contact. Figure 2B shows the surface platelets forming nodular botryoidal structures of turquoise-green copper sulphates (EDX Cu, S, O). The crystals are tentatively identified as brochantite, awaiting micro-XRD studies.

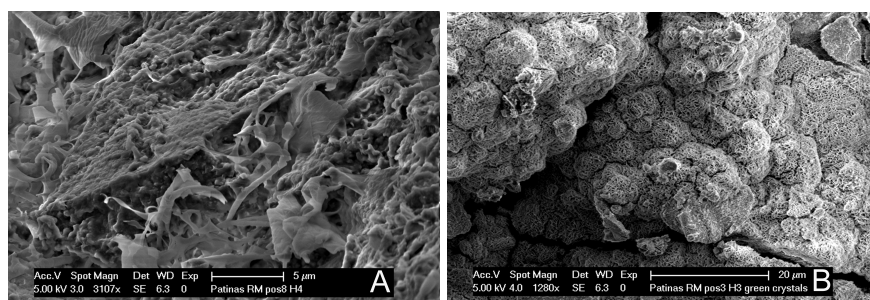


Figure 2

SEM of mounted microsamples taken from the hair of *Hercules Pomarius*. (A) shows the intricate net of wax crystals on the outside of the patina layers; (B) shows the nodular botryoidal crystal growth of green copper sulphates. These nodules are shown in cross section in Figure 3

Imaging chemical microscopy

Figure 3 (top) shows a back-scattered electron (SEM-BSE) image of a polished cross section of hair from *Hercules Pomarius*. The highly back-scattering electron layer at the bottom represents the metal bearer (yellow in light microscopy/LM). The next, somewhat unstructured, primary layer contains gypsum particles (low BSE) and zinc containing mineral fractions with medium BSE (dark greenish brown in LM). On top, secondary multilayered botryoidal structures (dark brown in LM) with a high BSE are seen, which correspond to the nodular crystals shown in Figure 2B. Figure 3 (bottom) is a more detailed view into the layered structure of these nodules. Higher up, a third layer is present with mainly sharp-edged fragments from the secondary layer and other minerals packed in an organic matrix (dark brown in LM). This layer is considered to be a weathering and conservation layer. The botryoidal structures suggest a slow growth process. Similar structures were observed on a group of bronze figures – *Hercules*, *Nessus* and *Deianeira* (BK-1957-2) c. 1850 – cast by Charles Crozatier, so it is not a typical 17th-century patina feature but rather an authentic mineralization layer build with metal ions diffusing into an early patina layer architecture.

The low-resolution BSE and EDX map of a selected area in the cross section in Figure 3 are shown in Figures 4A to 4C. Figure 4B combines

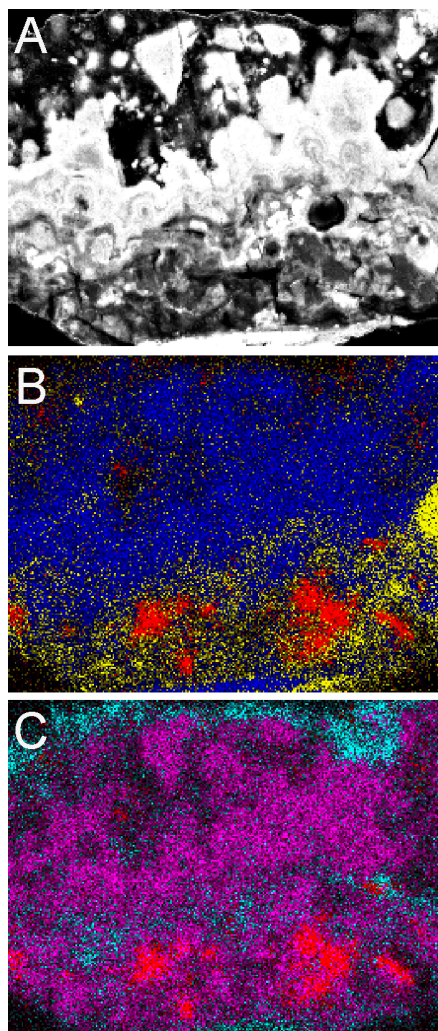


Figure 4
SEM-EDX maps of the polished cross section of *Hercules Pomarius* shown in Figure 3: (A) low-resolution BSE corresponding to (B) the copper (blue), zinc (yellow) and calcium (red) map and (C) the calcium (red), sulphur (purple) and chlorine (light blue) map

the distributions of copper (Cu K-line; dark blue), zinc (K-line; yellow) and calcium (K-line; red). Figure 4C combines the distributions of chlorine (K-line; light blue), calcium (K-line; red) and sulphur (K-line; purple). Calcium-intense spots show high peaks for sulphur and oxygen, pointing to gypsum. Copper is present in all the patina layers. Sulphur, copper and oxygen are most concentrated in the banded high BSE botryoidal structures, possibly brochantite. Zinc, mostly concentrated adjacent to the bronze in an unknown molecular form, migrated, pointing to dezincification of the bronze (Scott 2002). Chloride may play a role in the mobility of the metal ions. A high BSE layer of precipitates with copper and chloride could point to atacamite. The zinc and copper both migrated from the bronze into organic layers that turned into metal soaps (see below). Spot analysis of the low BSE part of the top layer shows higher concentrations of chlorine next to carbon (high intensity), sulphur, oxygen, copper, calcium, iron and virtually no zinc. Other samples from the hair also show chaotic carbon-rich layers with quartz and clay minerals.

Figure 5 shows four FTIR maps overlain using Photoshop on the corresponding SEM-BSE picture, employing the outer circumference given by the embedding resin FTIR carbonyl map at 1730 cm^{-1} (Figure 5A). The false colour represents a thermal colour scheme ranging from high intensity (red) to low intensity (blue). The images are taken in reflection mode with instrumentation and methodology described by Van der Weerd et al. (2004). The CH vibrations of fatty substances like waxes and fatty acids at 2900 cm^{-1} (Figure 5B) are strongest in the organic-rich top layer of the composite. Metal soaps summarized between 1520 and 1616 cm^{-1} (Figure 5C) peak and overlay the secondary zone with the botryoidal features of the copper sulphates. The sulphates also peak in the botryoidal zone, but extend to the primary layer as well, where gypsum is present (Figure 5D).

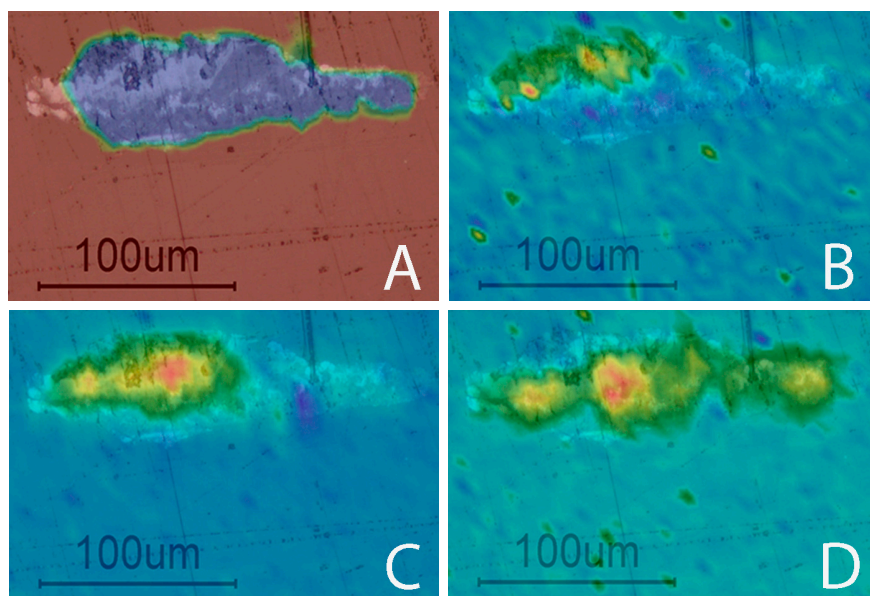


Figure 5
Imaging FTIR microscopy maps overlain on the SEM image of the hair of *Hercules Pomarius* (Figure 3). (A) embedding resin image at 1730 cm^{-1} outlining the cross section; (B) image of CH vibrations at 2900 cm^{-1} from fatty substances; (C) image map of metal soap carboxylate absorptions from 1520 – 1616 cm^{-1} ; (D) image map of sulphate absorptions from 1086 – 1218 cm^{-1}

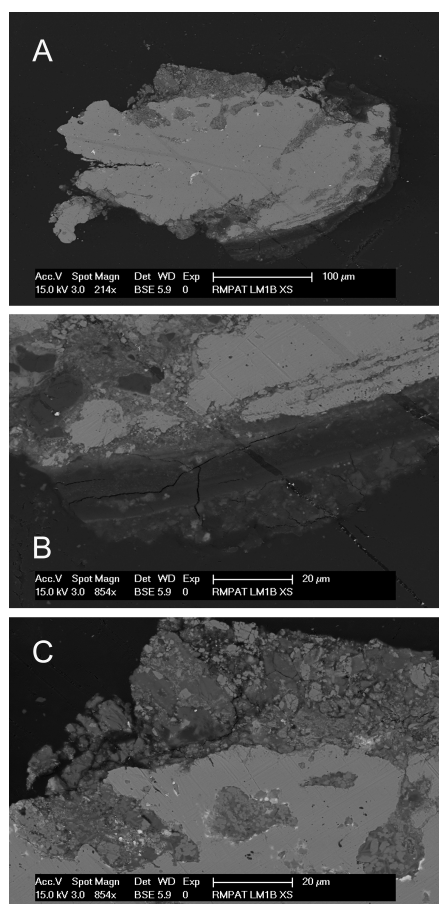


Figure 6

SEM-BSE images of the bronze and patinas from *Striding Warrior* (BK-1959-3). (A) is an overview of the polished section; (B) shows the lower right corner of the sample where low BSE organic layers are discordantly applied over a particle-rich primary layer (detail is SW in A); (C) shows a detail of A with the primary patina layer in direct contact with the metal (detail is NW in A)

The correlation of metal soaps, sulphates and copper point to a primary metal-soap structure of copper and oil-derived fatty acids that mineralized into banded nodular structures of copper sulphate. The blue-green prismatic mineral brochantite is known to develop into these botryoidal features in copper ores (Stevko et al. 2011). This secondary feature of the patina must have developed from an organic layer applied originally as an oily animal fat, which is suggested by the presence of myristic, palmitic and stearic acids in the DTMS. Metal soaps develop over time when biological ester bonds of the triglycerides hydrolyse and bond with metal ions (Keune and Boon 2007). Sulphides have been used as a reactant to develop mineralized chemical structures (Corkery 1998). Introduction of sulphides is a common practice in patination and may well have been used in the 16th or later centuries (Hughes and Rowe 1991). Alternatively, sulphates can form by exposure to atmospheric SO_2 , as is the case on outdoor bronzes (Scott 2002). The layer lying directly on the bronze contains gypsum particles and unknown phases of copper and zinc reacted with oxygen, sulphur and chlorine. Its binding is presently unknown but could be revealed with imaging SIMS studies. The FTIR maps suggest that metal soaps could be present there also. Near the point of contact with the banded structure, high BSE particles are observed that coincide with copper, chlorine and sulphur-containing phases.

PATINA ON THE *STRIDING WARRIOR*

Imaging chemical microscopy

The patina on *Striding Warrior* has a different, more greenish lustre. The patina buildup is shown as SEM-BSE images (Figures 6A to 6C). The bulk of the sample is bronze with traces of tin and lead (high BSE aggregates). The sampling of the metal was unintentional. The metal shows a circumference with many open 'valleys' giving it an almost leached, corroded aspect (see also Figure 8). This aspect is expected for unchased bronze after the cast. An area of hair is difficult to chase. The patina has two different structures. On and partly inside the openings in the metal, a non-structured layer is visible with a broad spectrum of particle sizes and homogenous material. In the lower right corner, two very low BSE, and thus presumably organic, layers are discordantly applied over this primary patina layer. Figure 6B shows these layers at higher magnification. These were considered to be of much younger age. The chaotic primary patina in Figure 6C has an average elemental composition of oxygen and zinc with minor amounts of carbon, aluminium, silicon, calcium, sulphur, iron and copper. The bulk of the medium BSE particles contain Zn and O with some iron, pointing to a red-tinted zincite (dark red colour in LM). In between these particles, calcium, iron, chlorine, oxygen and sulphur-containing phases are present. The *Striding Warrior* patina is chemically oxygen dominated since the relative amount of sulphur is very low compared to the *Hercules* patina. The high BSE spots where the metal and patina come into contact are from lead metal. Tin is present as a trace metal in the bronze, but is also present in distinct areas outside the bearing metal. DTMS was not performed on this specific patina sample, but embedding of related samples resulted in extensive dissolution in the embedding

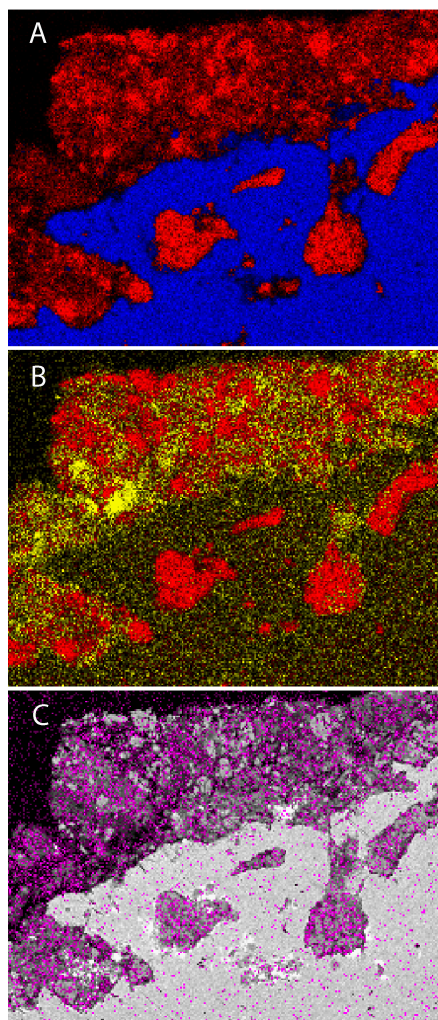


Figure 7
Energy-dispersive elemental maps of the primary patina with metal shown in Figure 6C. (A) combines the distribution of zinc (red) and copper (blue); (B) combines the distribution of zinc (red) and calcium (yellow); (C) is an overlay of the BSE map and iron (purple)

medium. EDX of remaining parts showed low BSE areas with carbon as a main element. Elsewhere on the statuette in the scrotum, DTMS showed a Gaussian profile of alkanes up to C50 (typically petroleum derived), fatty acids pointing to stand oil, cross-linked oil and some lead possibly used as a drier.

Elemental distribution maps are shown in Figures 7A, B and C. Figure 7A is the map of zinc (red) and copper (blue). Figure 7B is the map of calcium (yellow) and zinc (red). Figure 7C is the map of iron overlain on the BSE image. The distribution of the primary patina is chaotic and without any structure that would point to a slow growth and structural development comparable to the buildup on the *Hercules Pomarius* patina. Another important difference is the low relative amount of copper and sulphur. The authors conclude, therefore, that the original patina of the *Striding Warrior* has probably been removed and replaced by the present one with additional paraffin layers applied later on.

X-ray tomography

This same patina sample was subjected to x-ray tomography (XTM) to investigate the internal structure and the contact between metal and patina. This was a pilot study to see if XTM should be part of an analytical strategy in an early part of an investigation.

Embedding medium was thinned in order to be able to mount the sample on 500-micron-diameter steel pins. The sample was analysed with monochromatic x-rays of 30 KeV on the TOMCAT beamline at the SLS synchrotron². Tomographic data at a special resolution of 350 nm were obtained by rotation through 180° over a period of about two hours. Figure 8 shows a series of vertical xz sections through the middle of the elongated sample. The flatness at the base is due to the polishing to obtain SEM data (shown in Figures 6–7) prior to the XTM. The white, spotty areas are interpreted as lead inside the bronze mass. The darker grey areas are from patina squeezed in between the nooks and crannies of the cast metal, giving it a rather open structure at the surface where patina material can accumulate later on. The series shown in Figures 8A to 8B is from section 310 to 350 with 3.5-micrometer intervals, each equivalent to ten virtual section intervals. In general, this tomographic approach should precede further imaging studies of the sample. It is entirely obvious that there is not one typical cross-sectional plane. Even in such a small fragment (the bottom flat section is about 320 micrometres), one notices the great variety of geometric differences, with large cracks in the

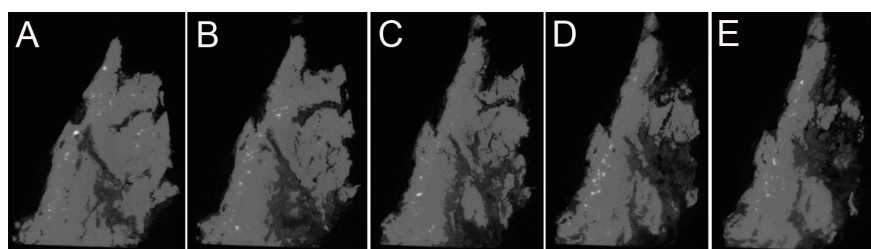


Figure 8
Virtual sections obtained from the x-ray tomographic data set of a hair sample from *Striding Warrior* showing the complexity of metal and patina even in microsamples. The 350 nm-thick sections are selected with a spacing by 3.5 micrometre

metal and differences in thickness of the patina. The present resolution of the XTM limits observation of details in the patina architecture. Further processing of the sample requires the selection of a scientifically interesting plane that must be reached by re-embedding of the sample and oriented sectioning and polishing.

CONCLUSION

The patinas of two 16th-century bronze statuettes were found to be extremely complex multilayer systems rich in information on the initial and later chemical events that led to a stable present-day layer. The upper-surface layer of a complete stratigraphy obtained from the 'landscape' of the hair shows that the latest layers are more chaotic and result from the application of waxy layers, whereas early layers show evidence of a slow buildup involving mineralizing metal-soap layers.

NOTES

- ¹ MOPAS is a device to steady the embedded sample during polishing.
- ² The Swiss Light Source (SLS) at the Paul Scherrer Institute is a third-generation synchrotron light source.

REFERENCES

- BOON, J.J.** 1992. Analytical pyrolysis mass spectrometry: New vistas opened by temperature-resolved in-source PYMS. *International Journal of Mass Spectrometry and Ion Processes* 118/119: 755–787.
- CORKERY, R.W.** 1998. *Artificial mineralisation and metallic soaps*. PhD thesis, Australian National University, Canberra.
- HUGHES, R. and M. ROWE.** 1991. *The colouring bronzing and patination of metals*. New York: Watson-Guption Publications.
- KEUNE, K. and J.J. BOON.** 2007. Analytical imaging studies of cross-sections of paintings affected by lead soap aggregate formation. *Studies in Conservation* 52: 161–176.
- PITTHARD, V., R. STONE, S. STANEK, M. GRIESSER, C. KRYZA-GERSCH, and H. HANZER.** 2011. Organic patinas on Renaissance and Baroque bronzes: Interpretation of compositions of the original patination by using a set of simulated varnished bronze coupons. *Journal of Cultural Heritage* 12: 44–53.
- POPE-HENNESSY, J.** 1965. *Renaissance bronzes*. London: Phaidon Press.
- SCOTT, D.A.** 2002. *Copper and bronze in Art: Corrosion, colorants, conservation*. Los Angeles: Getty Publications.
- ŠTEVKO, M., J. SEJKORA, and P. BACIK.** 2011. Mineralogy and origin of supergene mineralization at the Farbište ore occurrence near Poniky, central Slovakia. *Journal of Geosciences* 5: 273–298.
- VAN LANGH, R.** 2012. *Technical studies of Renaissance bronzes*. Amsterdam: Rijksmuseum.
- VAN LANGH, R., E. LEHMAN, S. HARTMANN, A. KAESTNER, and F. SCHOLTEN.** 2009. The study of bronze statuettes with the help of neutron imaging techniques. *Analytical and Bioanalytical Chemistry* 395: 1949–1959.
- VAN DER WEERD, J., R.M.A. HEEREN, and J.J. BOON.** 2004. Preparation methods and accessories for the infrared spectroscopic analysis of multi-layer paint films. *Studies in Conservation* 49: 193–210.

How to cite this article:

Boon, J.J. and R. van Langh. 2014. Comprehensive studies of patinas on Renaissance bronze statuettes with laboratory, synchrotron and neutron-aided techniques. In *ICOM-CC 17th Triennial Conference Preprints, Melbourne, 15–19 September 2014*, ed. J. Bridgland, art. 0901, 7 pp. Paris: International Council of Museums. (ISBN 978-92-9012-410-8)